Digest Journal of Nanomaterials and Biostructures Vol. 18, No. 4, October-December 2023, p.1515-1527

Cetyl alcohol surface functionalization: a strategy for modulating electronic characteristics of boron nitride nanosheets

S. M. Neeraja*, B. Bindhu
Department of Physics, Noorul Islam Centre for Higher Education Kumaracoil, Thuckalay- 629 180, Tamilnadu, India

Hexagonal boron nitride (h-BN) is a two-dimensional material with a unique layered structure akin to Graphene. Cetyl alcohol ($CH_3(CH_2)_{15}OH$) denoted as CA, a fatty alcohol derived from natural sources like palm oil and coconut oil, holds a significant place in various industries due to its versatile properties. Cetyl alcohol's has a potential in forming stable nanostructures and its interactions with other compounds, shedding light on its utility in nanotechnology and materials science. In this work exfoliation of BNNS and subsequent functionalization using Cetyl alcohol is investigated. The functionalization of boron nitride nanosheets (BNNS) using CA is investigated in this study. The modification process aims to enhance the properties and applications of BNNS. OH groups are functionalized and bring about beneficial changes to its properties, enabling enhanced interactions with other compounds. This modification can lead to improved solubility, emulsification, and lubrication capabilities, expanding its utility in various applications such as cosmetics, pharmaceuticals, and industrial processes. Characterization techniques, including Thermogravimetric analysis(TG/DTA), UV-Visible spectroscopy, Photoluminescence, X- ray diffraction (XRD), Raman spectroscopy, Fourier transform infrared spectroscopy (FTIR) are employed to analyze the efficacy of the functionalization process. Thermogravimetric-differential thermal analysis (TG-DTA) was utilized to investigate the thermal characteristics of the functionalized samples.

(Received September 20, 2023; Accepted December 8, 2023)

Keywords: Boron nitride nanosheets, Exfoliation, Cetyl alcohol, Surface functionalization, Electrical applications

1. Introduction

The demand for two-dimensional (2D) nanomaterials has emerged as a crucial necessity within the framework of sustainable development. These nanomaterials, characterized by their ultra-thin structures and unique properties, offer a myriad of opportunities to address pressing global challenges while minimizing environmental impact.

Firstly, 2D nanomaterials exhibit remarkable mechanical, electrical, and optical properties that can revolutionize various industries. Their high surface area to volume ratio enhances catalytic efficiency, facilitating cleaner and more energy-efficient processes in sectors such as energy production and storage [1]. This, in turn, reduces resource consumption and pollution, contributing to sustainable energy solutions.

Furthermore, 2D nanomaterials enable advancements in water purification and environmental remediation. Their high adsorption capacities and tailored surface properties facilitate efficient removal of pollutants from water and air, mitigating the detrimental effects of pollution on ecosystems and human health [2]. Additionally, the integration of 2D nanomaterials in electronics and sensors enhances the precision and efficiency of data collection, leading to smarter resource management and reduced energy consumption. This, coupled with their potential in nanomedicine, opens avenues for sustainable healthcare solutions and improved drug delivery systems.

* Corresponding author: neerajasm11@gmail.com
https://doi.org/10.15251/DJNB.2023.184.1515

Two-dimensional (2D) materials have emerged as a fascinating class of substances with remarkable properties and diverse applications. Unlike their bulk counterparts, 2D materials possess an ultra-thin, single-layer structure that leads to intriguing quantum and size effects.

One prominent example of such a material is hexagonal boron nitride (h-BN), which has garnered significant attention due to its unique characteristics. Material is well known for its excellent insulating properties, high thermal conductivity, and chemical stability. It serves as a versatile substrate for other 2D materials and finds applications in electronics, photonics, and even quantum technologies.

Unlike its close counterpart Graphene, h-BN is an insulator rather than a conductor. This insulating behavior, while advantageous in certain applications, restricts its direct use in electronics and other electronic-related fields where high electrical conductivity is required. Additionally, while h-BN exhibits excellent thermal conductivity, it falls short of surpassing the remarkable thermal properties of materials like Graphene. This limitation, although not severe, can influence its effectiveness in certain thermal management applications. In summary, while hexagonal boron nitride offers a range of remarkable attributes, including thermal stability, chemical inertness, and excellent dielectric properties, its limitations in terms of electrical conductivity, thermal conductivity compared to Graphene, synthesis scalability, and potential reactivity under extreme conditions must be taken into account when considering its applications [3]. Researchers continue to explore strategies to overcome these limitations and unlock the full potential of h-BN in various technological realms.

Cetyl alcohol, a fatty alcohol derived from natural sources such as palm oil or coconut oil, holds a significant place in various industries due to its versatile properties and wide-ranging applications. With a long hydrocarbon chain, CA exhibits characteristics that make it valuable in both cosmetic and industrial formulations [4]. It serves as an emulsifying agent, aiding in the stabilization and blending of diverse ingredients in skincare and personal care products. Furthermore, Cetyl alcohol's lubricating properties find utility in industrial processes, enhancing the smooth operation of machinery and reducing friction [5]. Beyond its role as an emulsifier and lubricant, CA contributes to the formation of stable nanostructures, holding promise for applications in nanotechnology and materials science. It can modify surface properties, leading to enhanced interactions with other compounds and facilitating diverse chemical processes [6].

The present work focuses on the functionalization of BNNS using cetyl alcohol. Functionalization of BNNS using CA presents a significant avenue for tailoring their properties and expanding their applicability. In the realm of nanotechnology, functionalized BNNS can find use in nanocomposite fabrication, enhancing the compatibility and interactions between the nanosheets and polymers. Moreover, the functionalization of BNNS using CA can enhance their dispensability in solvents, making them more amenable to various processing techniques. This, in turn, facilitates the incorporation of BNNS into coatings, films, and other products, thereby expanding their potential applications.

In conclusion, the functionalization of boron nitride nanosheets using cetyl alcohol represents a strategic approach to customizing their properties and augmenting their utility across a diverse range of industries and technological domains.

2. Materials and methods

2.1. Materials

All the materials used in the study are supplied by Sigma Aldrich. BN powder (Molecular Weight=24.82 g/mol, particle size~1µm, density=2.29 g/mL at 25^{o}C), Cetyl alcohol (Molecular Weight= 242.41g/mol, density= 0.810g/mL at 25^{0}C), De-ionized water, Acetone and DMF by Merck specialist India.

2.2. Exfoliation of BNNS using DMF and functionalization using Cetyl alcohol

In order to remove any traces of moisture, an appropriate quantity of BN was obtained and heated at an average temperature of 800°C. To ensure even distribution, the heated BN powder was introduced into the organic solvent DMF and vigorously stirred for approximately 15 minutes.

The resulting solution was then subjected to ultra-sonication using a probe sonicator for an hour, resulting in exfoliated BN nanosheets. The solution was centrifuged at 3000 rpm to remove any remaining un-exfoliated particles. After a wash with deionized water, the isolated particles were dried in an 80°C oven for a full day. The dried material was subsequently powdered through grinding and functionalized using CA. Cetyl alcohol is soluble in acetone, 1g of CA is added to 50 ml of acetone and solution is formed.

0.2g of BNNS is added to 50ml of water and prepared CA solution are added the mixture is stirred for a duration of 4 hours, resulting in the formation of a white fluffy solution (solution of BNCA1) another 0.2g of BNNS is combined with 50ml of DMF, and the prepared CA solution is added and stirred to yield a pale blue solution (solution of BNCA2). The solutions obtained undergo ultra-sonication and subsequent centrifugation. The resulting particles are dried in a hot oven at 80°C for 24 hours to yield BNCA1 and BNCA2.

3. Characterization

Powder X-ray diffraction analyses were conducted employing an X-PERT-PRO X-ray diffractometer with Cu kα radiation (λ = 1.5406 Å), operating at 30 mA and 40 kV. The XRD technique enabled the examination of the phase structure of the prepared samples. Additionally, Thermogravimetric Analysis (TGA) was performed using a PerkinElmer Diamond instrument under a nitrogen atmosphere**.** FTIR spectroscopy analysis was conducted using a FTIR spectrometer (Bracker Alpha). Raman analysis was accomplished using a JYHR-800 Raman spectrometer, with sample excitation using a 488 nm argon ion laser instrument. Photoluminescence studies were carried using Varian Cary Eclipse Photo Luminescence Spectro photometer. UV- visible spectrum was conducted UV-DRS-Spectrophotometer, Thermo fisher Evaluation 220.

4. Results and discussion

4.1. XRD

The powder sample undergoes X- ray diffraction studies which involve analyzing the diffraction patterns generated when X-rays are scattered by the crystalline structure of BNNS. This technique provides valuable information about the material's crystallographic properties, such as its lattice parameters, crystal size, and orientation. The X-ray diffraction spectra of BNNS, BNCA1 and BNCA2 are illustrated in fig 1. The distinctive peak for exfoliated BN emerges at 26.620^0, aligning with the (002) crystallographic planes of h-BN (JCPDS card number-34-0421) [7], while minor peaks manifest at 41.590^0 and 54.942^0. Upon subjecting BNNS to Cetyl Alcohol, additional peaks become evident. Figure 1(b) of BNCA1 illustrates peaks at 21.67^0, 24.616^0, 26.926^0, 36.351^0, 40.366^0, 41.836^0, 43.937^0 while figure 2 (c) of BNCA2 reveals peaks at 21.466^0, 24.826^0, 26.926^0, 36.352^0, 40.3532^0, 41.836^0, 44.146^0, additional peaks signify the presence of Cetyl alcohol. The slender yet distinct peak observed in the BNCA nanocomposite indicates the restoration of the crystalline nature of BNNS.

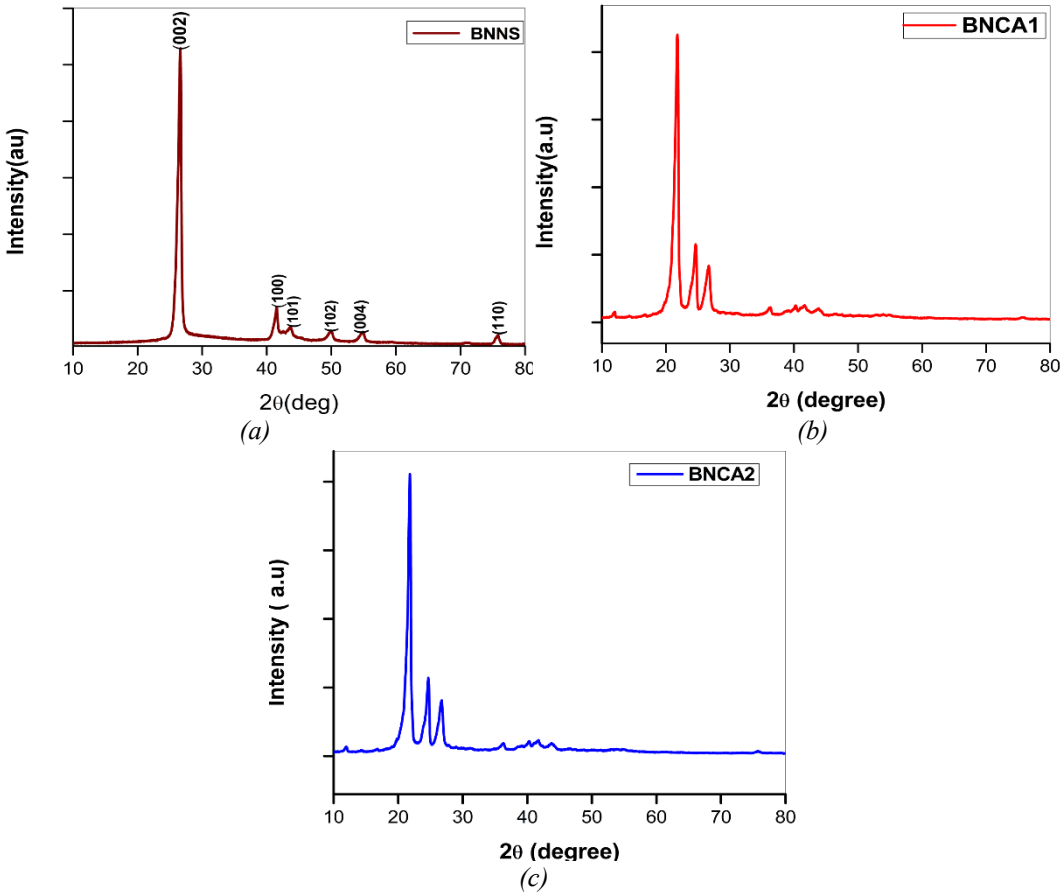

Fig 1. XRD Spectrum of (a)BNNS, (b)BNCA1, (c)BNCA2.

The introduction of functionalized BNNS results in a peak appearing at 26.68^0, indicating a change compared to the BNNS baseline. This change is linked to the existence of hydroxyl groups located on BN sites, which can change the chemical reaction and interactions of nanosheets. The O-H group can provide site for further chemical reaction making it possible to attach other functional groups or molecules to the surface. O-H group functionalization using Cetyl alcohol, due to the presence of large no of O-H groups it increases the dispensability of BNNS in solvent. Cetyl alcohol functionalized BNNS also improves the interfacial adhesion in the polymer and other materials, thus enabling the usage of this prepared material in many applications.

Interplanar spacing (d), of the crystal lattice BNNS, BNCA1, BNCA2 were calculated using Braggs law,

$$n\lambda = 2d\,\mathrm{Sin}\theta \qquad (1)$$

where λ represents the X-ray wavelength employed (1.540569 A˚) and are denoted (Table 1).

Table 1. Interplanar spacing (d) for different 2θ values.

Sample	2θ	d- spacing(A^0)
BNCA1	21.67	4.0965
	24.616	3.583
	26.926	3.308
	36.351	2.471
	40.366	2.236
	41.836	2.157
	43.937	2.067
BNCA2	21.466	4.1361
	24.826	3.583
	26.926	3.308
	36.352	2.467
	40.3532	2.232
	41.836	2.157
	44.146	2.040

The lattice parameters of the BNCA1, BNCA2 samples were displayed in Table 2. Consequently, these calculated lattice parameters aligned with the established JCPDS data. There is a slight change in calculated lattice parameter values while comparing with standard values. This may be due to stress, and introduction of newer materials to the crystal lattice. The addition of Cetyl alcohol for surface functionalization causes small lattice distortions, those results in changes in lattice parameters

Table 2. Representation of crystal lattice parameters of the prepared samples.

	Lattice parameter	
Sample	Standard value (A^0)	Calculatedvalue (A^0)
BNCA1	a =b =2.504 c = 6.656	a = b = 2.157 c = 7.166
BNCA2		a = b = 2.157 c = 6.616

4.2. Williamson–Hall (W-H) plot

Fig 2 shows Williamson hall plot of BNNS, BNCA1,BNCA2 respectively. From W-H plot the crystal size of BNNS is 20.8069 nm and the corresponding lattice strain is found to be 5.57, for BNCA1 crystal size is 27.6895 nm and the lattice strain is found to be 8.23 and for BNCA2 crystal size is 17.617 and their corresponding lattice strain is found to be 3.18.

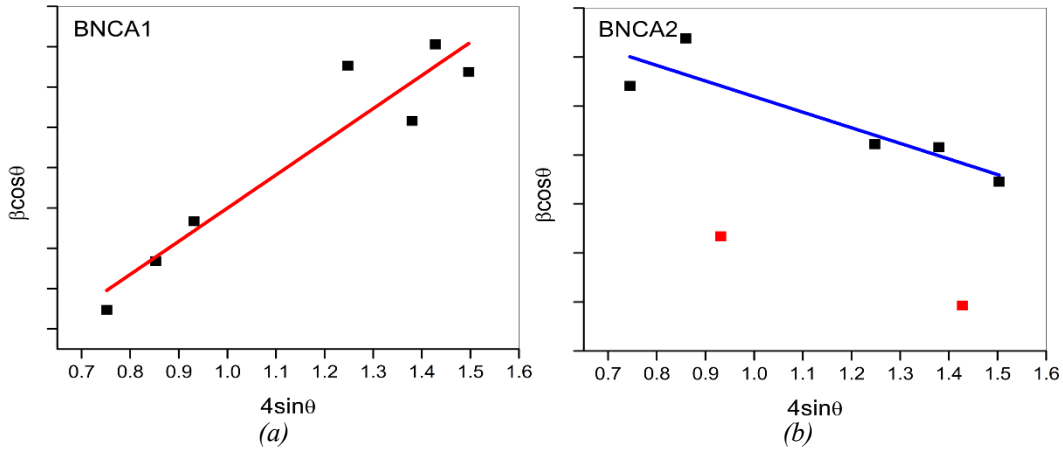

Fig. 2. Williamson-Hall (W-H) plot of (a) BNCA1, (b)BNCA2.

Functionalization of BNNS with Cetyl alcohol in DMF solvent (BNCA2) results in decrease in crystalline size as the hydrophobic alkyl chain of Cetyl alcohol attaches to the surface of BNNS thus enhancing the dispersion and stability of nanosheets in DMF. These alkyl chains create a protective layer around BNNS reducing the surface defects and lattice strain itself. In the case of BNCA2 there is an increase in lattice strain with increase in crystalline size. As the nanosheets have the tendency to agglomerate to larger crystalline domains thus enhancing stronger interaction between sheets that led to aggregated structures involving high lattice strain.

4.3. FTIR

The Fourier Transform Infrared (FTIR) analysis was performed on BNNS, BNCA1, and BNCA2, in the spectral range of 400-4000cm^{-1}. The corresponding results are shown in Fig 3(a), 3(b), and 3(c) for each material, respectively. Distinctive peaks appear at 813.85cm^{-1} and 1384.70cm^{-1} for exfoliated BNNS.

From fig 3(b) BNCA1 shows characteristic peaks at 2919 cm^{-1}, 2846.23cm^{-1}, 2359.76cm^{-1}, 1393.62cm^{-1}, 1058.98cm^{-1}, 803.66cm^{-1}, 718.30cm^{-1}.While FTIR spectrum of BNCA2 shows eminent peaks at 3332.70 cm^{-1}, 2919.50cm^{-1}, 2846.23cm^{-1}, 1387.58cm^{-1},1064.56cm^{-1}, 803.66cm^{-1}, 721.28cm^{-1}. The eminent peaks are observed at 803.66cm^{-1} and 1393.62 cm^{-1} for BNCA1 and 803.66 cm^{-1} and 1393.62 cm^{-1} for BNCA2 provides valuable insights into the material's molecular composition and bonding similar to that of BNNS. All other characteristics peaks shows the surface functionalized BNNS using Cetyl alcohol**.** BNCA1 exhibited minor yet sharp peaks, while BNCA2 displayed more pronounced peaks in its FTIR spectrum, suggesting a higher degree of functionalization of boron nitride nanosheets through the use of DMF as the solvent.

The presence of minute, intense V-shaped peaks at 718.30cm^{-1} and 721.28cm^{-1} in figures 3(b) and 3(c), respectively, indicates the existence of B-N bonding among the atoms. Likewise, the occurrence of peaks at 1058.98cm^{-1} and 1064.56cm^{-1} demonstrates the B-N-O bonding between the nanosheets. The presence of a subtle U-shaped peak at 3332.70 cm^{-1} in Fig 3(c) indicates the manifestation of OH stretching vibrations from the hydroxyl group in the alcohol.

Symmetric stretching vibrations of C-H bonds are observed at 2919.50, 2846.23 and 2919.50, 2846.23 for BNCA1 and BNCA2 respectively. This peak corresponds to (CH_2) methylene groups in hydrocarbon chain of cetyl alcohol. The strong and prominent v-shaped peak at 1064cm^{-1} in BNCA2 signifies the stretching vibration of the carbon-oxygen (C-O) bond within the alcohol's hydroxyl group. Additionally, the presence of a C-O-C stretching is observed at 1387.58 cm^{-1}.

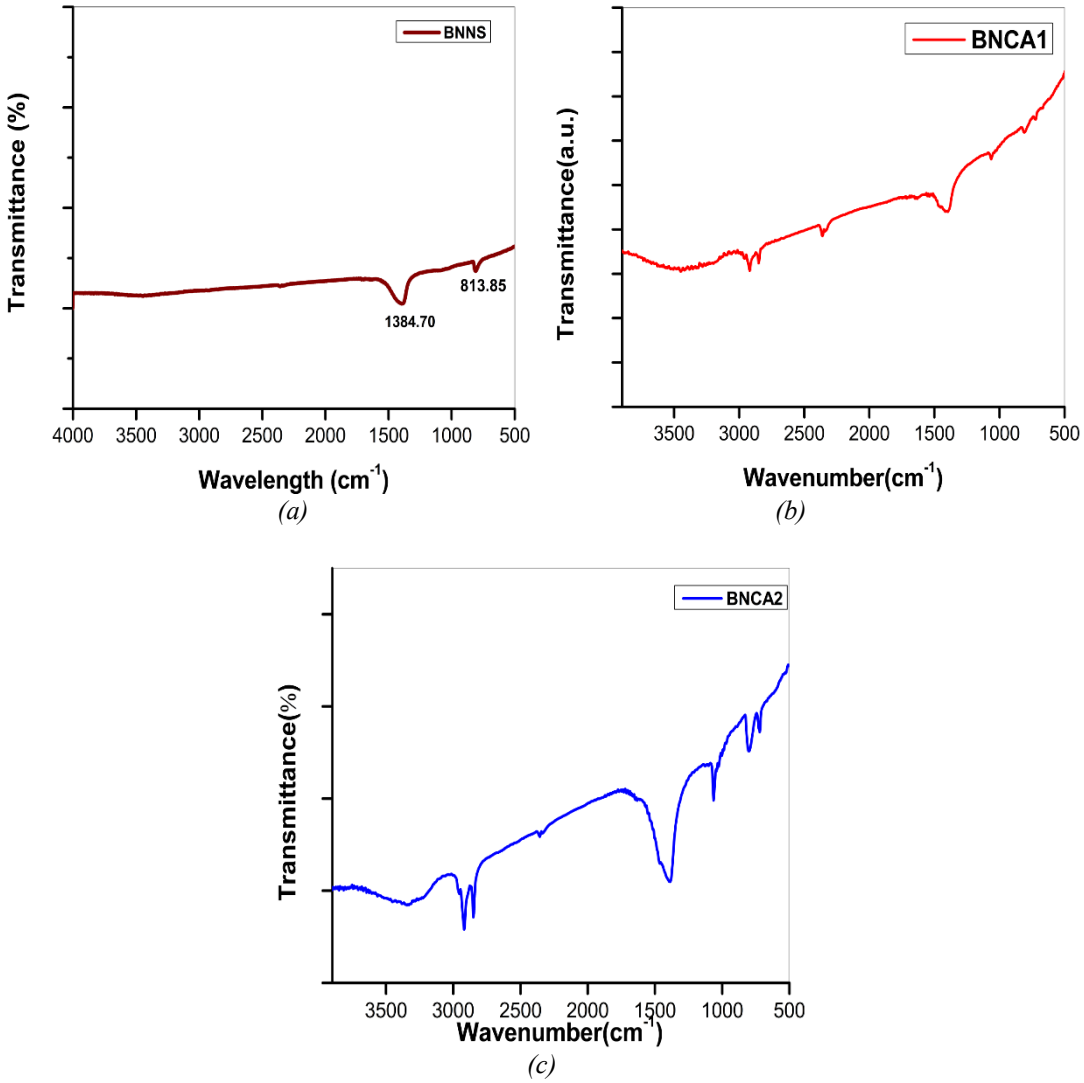

Fig. 3. FTIR Spectrum of (a)BNNS, (b)BNCA1, (c)BNCA2.

4.4. TG/DTA analysis

The TGDTA spectrum of BNNS, BNCA1, BNCA2 are shown in the fig 4 .TGA analysis is a common technique used to analyze the behavior of material. The TG curve shows the change in sample weight as a function of temperature or time. The onset degradation temperature is a critical parameter obtained from TGA analysis. It represents the temperature at which the sample begins to undergo significant thermal degradation. From the data presented in Fig 4, it is observed that the initiation of degradation for BNNS occurs at a temperature of 201.26°C, accompanied by an initial weight loss of 0.084%, followed by a subsequent loss of 0.43%.

Onset degradation temperature of BNCA1 is 167.96^{0}C (fig 4b) with a weight loss of 83.14% and that of BNCA2 is 152.62^{0}C with a weight loss of 82.92% At the beginning of weight loss curve 100^{0}C to 152^{0}C, weight loss remains relatively constant this initial stable region indicates that Cetyl alcohol functionalized BN nanosheets possess good thermal stability at lower temperature. As temperature continuous to raise the weight loss curve exhibit a gradual decrease in weight. This region corresponds to the initial decrease of Cetyl alcohol functionalized group attached to BN nanosheets. The most significations occur in this region (132.81^{0}C to 264^{0}C. Cetyl alcohol functionalized group further breakdown to smaller fragments. This stage often involves the release of more established amount of volatile gases, resulting in the pronounced decrease in the

sample weight. Towards the higher end of the temperature range the weight loss curve may start to level off indicates that the majority of organic components have been volatized and decomposed.

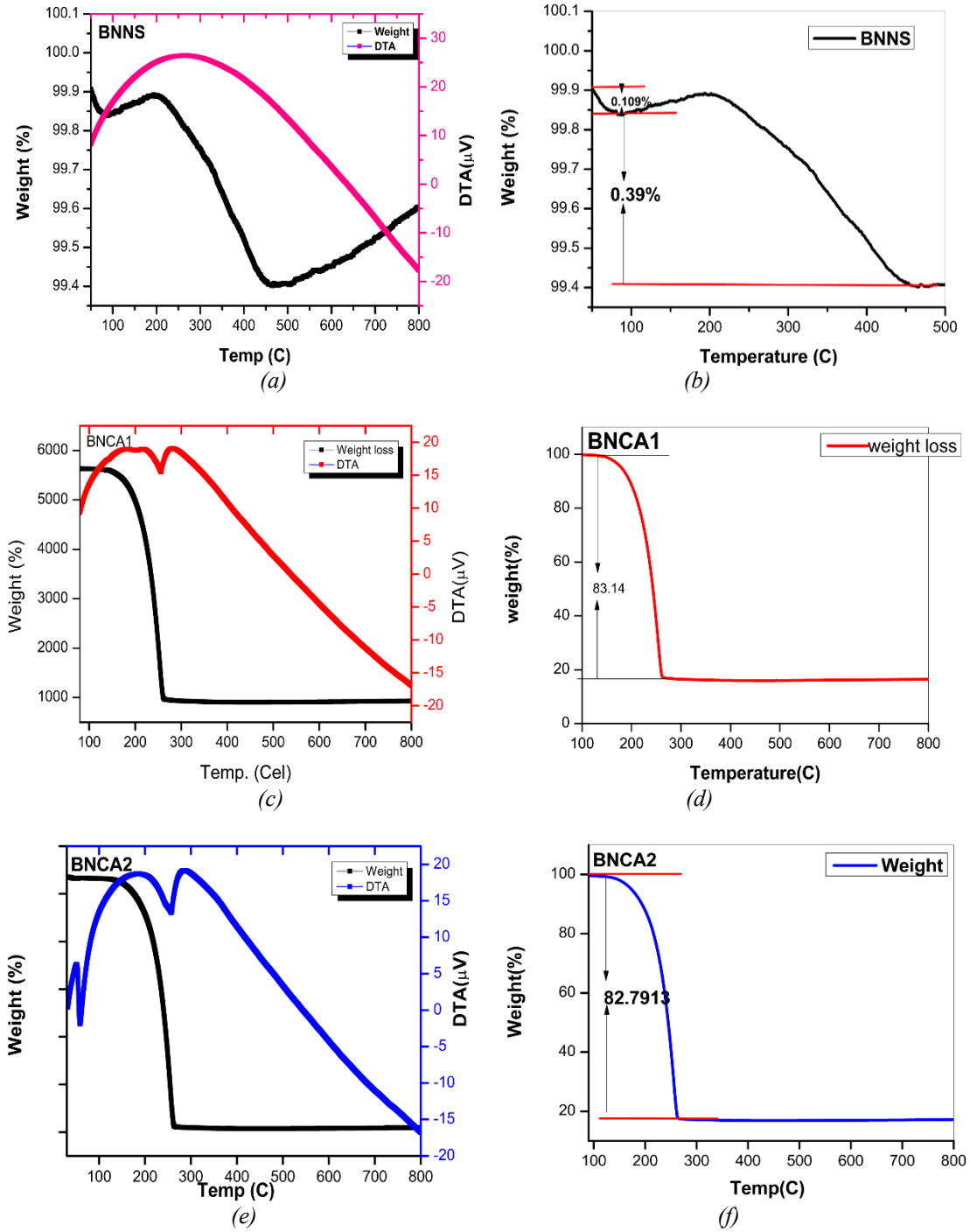

Fig. 4. TG-DTA analysis and Weight Loss curve of (a)BNNS, (b)BNCA1, (c)BNCA2.

Cetyl alcohol functionalized BNNS, the DTA curve depicts the heat flow as the material is subjected to increase in temperature. One of the primary reactions that can be inferred from DTA curve is functionalization of BNNS with Cetyl alcohol. This process involves bonding of Cetyl alcohol to the surface of BNNS, as the temperature increases the DTA curve might show an exothermic peak indicating the adsorption of heat during the chemical bonding process. There may

be other thermal event on the DTA curve such as decomposition of volatile component during the functionalization process which is exothermic in nature. The presence of both exothermic and endothermic reaction in the DTA curve provide insight to the energy change accompanied with the process occurring within in the Cetyl alcohol functionalized BNNS.

The DTA curve of BNCA1 have first endothermic peak at 217^0C and second at 283^0C. Initial weight loss is observed at first endothermic peak. Decrease in the rate of heat adsorption is observed at 256.57^0C. At the initial stages of DTA curve a small endothermic peak is observed and within 100^0C moisture content will be absorbed and endothermic reaction happens.

BNCA2 has more intense peak for exothermic reaction compared to BNCA1 as the temperature increase, a broad exothermic peak become evident on the DTA curve this exothermic peak can be attributed to the chemical reaction between Cetyl alcohol and the BNNS surface. The release of heat during this step indicates an exothermic reaction and that energy is being release as new chemical bonds are formed.

4.5. Raman spectroscopy

Interpreting the Raman spectrum of BN provides valuable insight into the vibrational, chemical and crystal structure of the material. These peaks arise due to the vibration of the B and N atoms within the crystal lattice.

The prominence of a strong peak in the Raman spectrum of BNNS is apparent from Fig 5(a). The occurrence of the E_{2g} mode of BNNS is identified at 1383.91 cm^{-1}. Within the hexagonal lattice, there exist vibrational stretching modes of both boron and nitrogen atoms in the plane.

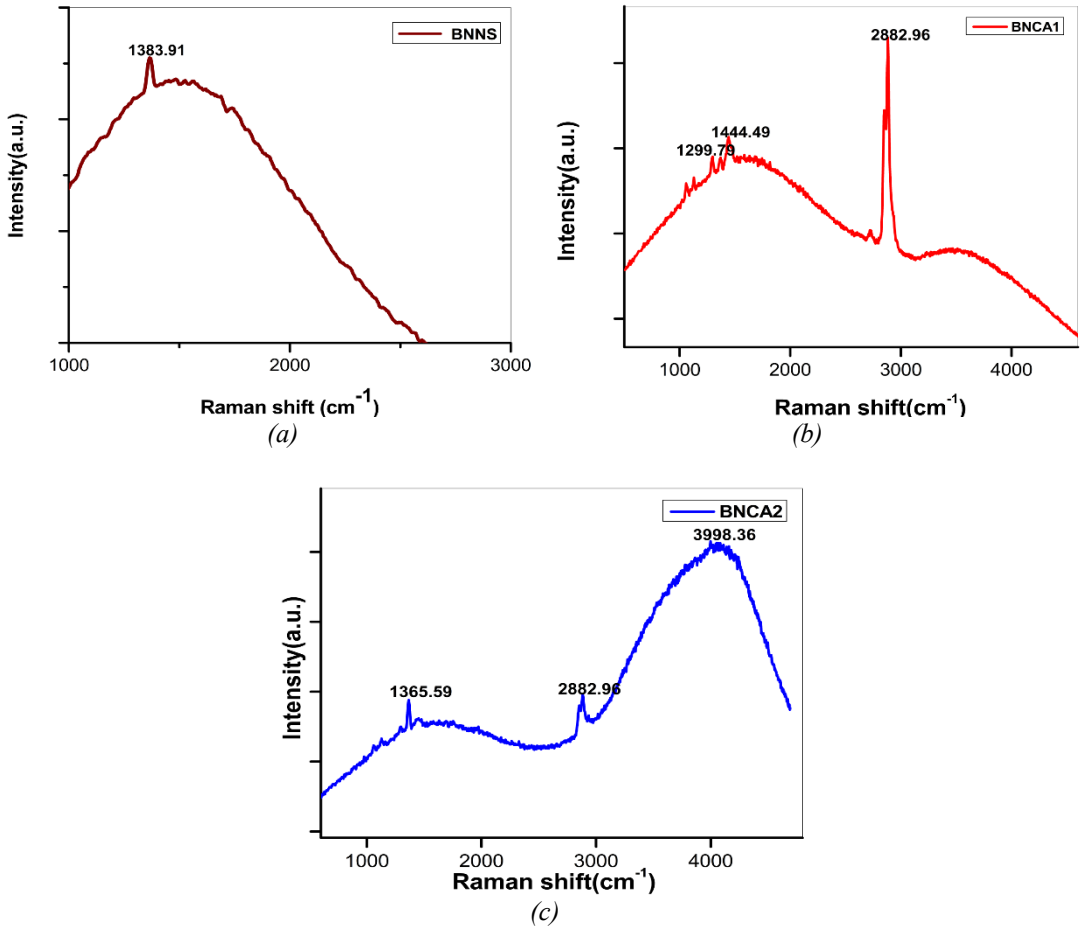

Fig. 5. Raman Spectra (a)BNNS, (b)BNCA1, (c)BNCA2.

For BNCA1 (fig 5(b)) a peak at 1367cm^{-1} indicates the crystalline quality of BN lattice. A red shift of 84.12cm^{-1} at 1299.79cm^{-1}.The peak signify the stretching vibration of the newly formed O-H bonds in the hydroxyl groups attached to the nanosheets surface. The observed peak corresponds to specific functional group like B-OH or N-OH indicating the successful attachment to the nanosheets. A intense at 1299.79cm^{-1} corresponds to C-O-C (ether) functional group This corresponds to stretching vibration of C-O bond in ether group because Cetyl alcohol contain an ether function group C-O-C in its nuclear structure. A intense peak at 1444.49cm^{-1} reveal the presence of -CH_2 bending vibration motion of the C-H bond in the alkyl chain of Cetyl alcohol molecules. The alkyl chain of Cetyl alcohol interacts with the BNNS surface through Vander waals forces and other interactions. This characteristic peak in Raman spectrum serves as the fingerprint of Cetyl alcohol functional group on BN nanosheets. At 2882.96 cm^{-1} a high intense peak depicts symmetric and asymmetric stretching vibration of CH2 groups and a blue shift is obtained.

The Raman spectra of BNCA2 are illustrated in fig 5(c). A small intense peak at 1365.59cm^{-1} communicates the CH_3- symmetric vibrations of Cetyl alcohol functional group as well as a red shift. Its peak is indicative of the alkyl CH_3 groups in Cetyl alcohol molecules. A very high intense peak at 3998.36cm^{-1} represents a blue shift and the O-H functional group. Stretching vibration of O-H group is key characteristic features of alcohol. The hydroxyl group attached to hydrocarbon chain in Cetyl Alcohol molecules gets functionalized on surfaces of BN nanosheets contribute observed Raman Peak. The peak at 3998.36cm^{-1} demonstrates a displacement towards higher wavenumbers, implying a blue shift. This shift signifies an augmentation in the vibrational frequency and reinforcement of the bond. Furthermore, it suggests enhanced interactions of Cetyl alcohol functional groups on boron nitride nanosheets than that of BNNS.

4.6. UV visible spectroscopy

The UV region of the spectrum (100-400 nm) provides information about the electronic transition involves the higher energy levels. Absorption peaks or bands observes in this region corresponds to electronic excitation across the band gap of the molecule. Fig 6(a), (b) and 7(a), (b) illustrate the UV spectra of BNCA1 and BNCA2, along with their respective Tauc plots. In the case of BNNS, the λ_{onset} value is 208.40nm, indicating an energy bandgap of 5.95eV [8]. From fig 6(a) a peak of significant intensity is noted at 260.73nm, while the associated λ_{onset} is determined to be 385.9nm, utilizing the energy-wavelength conversion equation.

$$E_g = 1240/\lambda_{onset} \quad (2)$$

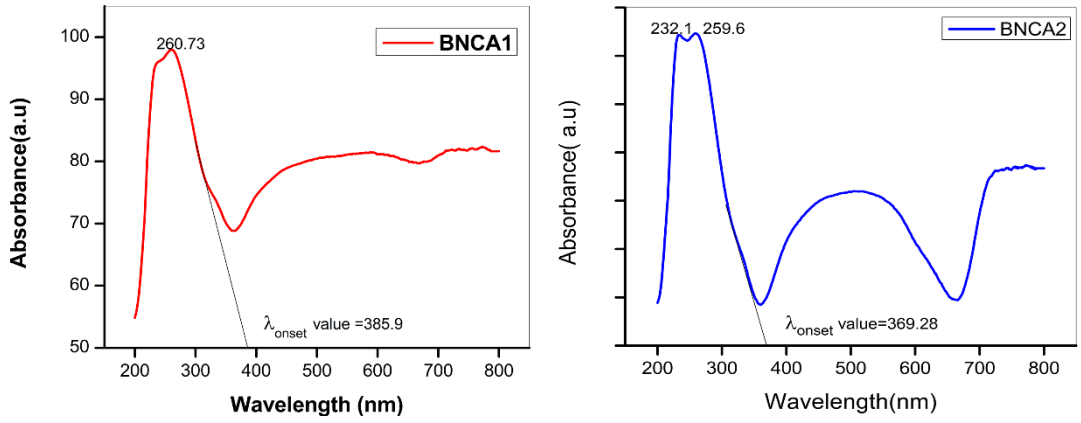

Fig. 6. UV-Vis spectra of (a))BNCA1 and (b)BNCA2.

The band gap is found to be 3.21 eV. In fig 6(b) high intensity peak is obtained at 232.1 nm and a corresponding λ_{onset} value is found to be 369.23nm and a band gap of 3.35eV is calculated.

The difference in energy levels between Cetyl alcohol functionalized BN & base BN nanosheets can be attracted to the effect of the functionalization on the electronic structure of the material. In the context of UV-Visible spectroscopy, the energy at which a peak occurs in the spectrum corresponding to the energy required for an electronic transition to the place. The peak at 3.21 eV for the Cetyl alcohol functionalized BN nanosheets indicates and electronic transition on that region with less energy compared to the peak at 5.95eV for base BNNS. It also enlightens the idea that the presence of Cetyl alcohol groups has introduced new electronic states or altered the energy levels within the material.

4.7. Bandgap determination using Tauc plot

Tauc plot in UV spectroscopy is to analyze and determine the optical bandgap energy of a material based on its absorption data.

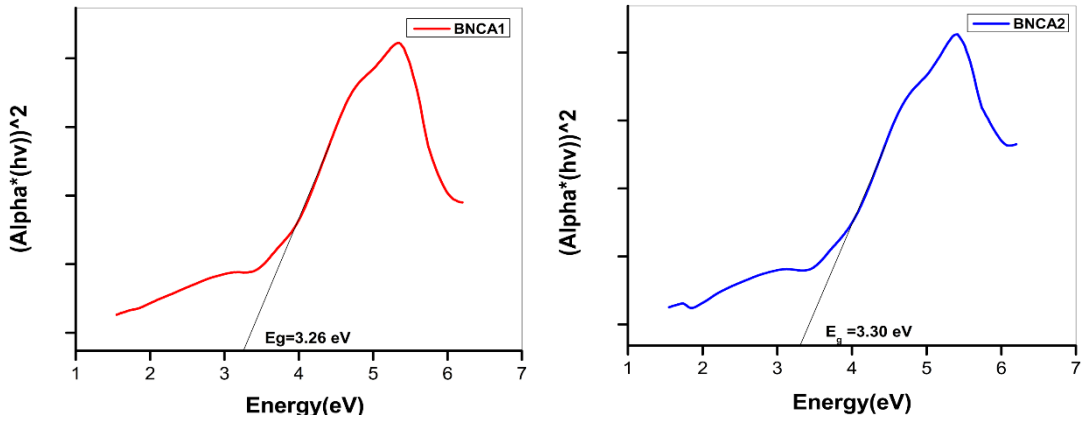

Fig. 7. Tauc plot of (a))BNCA1 and (b)BNCA2.

In Fig 7(a), it is evident that the band gap (E_g) for BNCA1 is 3.26 eV, while for BNCA2 (Fig 7b), the band gap is 3.30 eV. The energy band gaps derived from the Tauc plot align well with the calculated values. The introduction of Cetyl alcohol groups result in charge transfer between the functional group and nanosheet surface that lead to the change in band gap. Introduction of new surface state and defects in the nanosheet of BNNS alter the bad gap from 5.95 eV.

4.8. Photoluminescence (PL) analysis

The photoluminescence (PL) spectrum is a representation of the light emitted from a material after it has absorbed photons and undergone relaxation to lower energy states. The photoluminescence (PL) spectrum furnishes insights into the recombination process of electron-hole pairs and the subsequent emission of light as excited states return to their relaxed state.

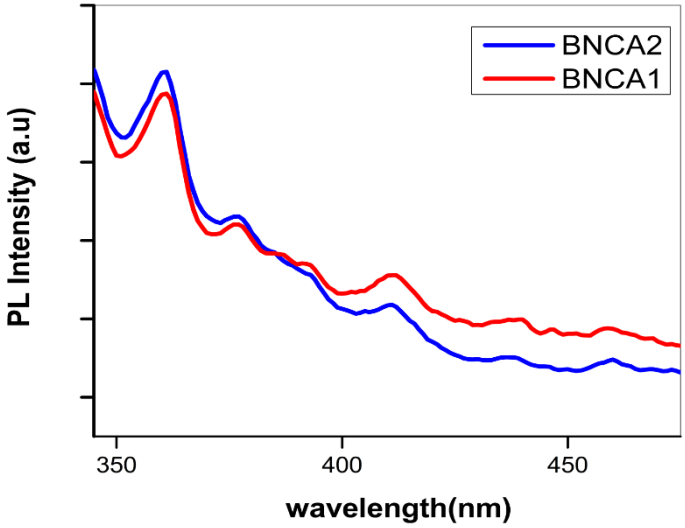

Fig. 8. PL Spectra of (a))BNCA1 and (b)BNCA2.

The PL spectrum of BNCA1 and BNCA2 is depicted in fig8. From the literature survey PL spectrum of BNNS shows DUV peaks at 224nm [9]. In the case of BNCA1 and BNCA2 (as shown in the fig 8), a prominent and intense peak is detected at 360.63 nm, corresponding to a band gap of 3.4 eV. There is a variation in intensity between the two prepared samples even though the bandgap remains unchanged. For BNCA1, the peak intensity measures 242.23 a.u., while for BNCA2, it registers at 256.22a.u. This is because the interaction between the Cetyl alcohol and the nanosheets could influence the electronic compiling between states involved in radioactive recombination, leading to change in the probability of light emission without affecting the bandgap.

5. Conclusion

The functionalization of boron nitride nanosheets (BNNS) using Cetyl alcohol has proven to be a significant and promising avenue for tailoring the properties of these nanomaterials. The successful modification process, as demonstrated through various characterization techniques, showcases the effectiveness of Cetyl alcohol in inducing surface changes and enhancing the dispensability of BNNS. From x- ray spectrum high intensive peaks were observed that confirms the crystallinity. Functionalization of BNNS with Cetyl alcohol in DMF solvent (BNCA2) results in a decrease in crystalline size thus enhancing the dispersion and stability of nanosheets in DMF. The determined lattice parameters are in accordance with the established JCPDS data from the XRD spectrum, indicating a consistent and reliable analysis of the material's crystal structure. Distinct functional groups within the prepared samples were discerned using FTIR spectroscopy.

Thermogravimetric (TG) and differential thermal analysis (DTA) were conducted to record and determine offset degradation temperatures. In comparison to BNCA1, BNCA2 exhibited a more pronounced exothermic peak for exothermic reaction as temperature increased. Notably, a broad exothermic peak emerged on the DTA curve, which is attributed to a chemical reaction between Cetyl alcohol and the surface of BNNS. Raman spectrum of BNCA1 and BNCA2 depicts red and blue shift, this shift indicates an increase in the vibrational frequency and strengthening of the bond. Moreover, it implies heightened interactions between CA functional groups and boron nitride nanosheets compared to BNNS. UV-visible spectrum analysis furnishes insights into the band gap characteristics, revealing that the band gaps of BNNS have been reduced from 5.95eV to 3.21eV and 3.35eV due to functionalization with BNCA1 and BNCA2. Notably, these values closely align with those derived from the Tauc plot analysis, providing robust evidence for the observed changes. The existence of Cetyl alcohol groups has introduced modified

the energy levels within the material. Photoluminescence (PL) results also show a reduction in the bandgap with pronounced intensity peaks, attributed to the successful and precise functionalization of BNNS using cetyl alcohol. The reduction in band gap leads to an improvement in electronic characteristics, rendering it suitable for electrical applications. Its altered electronic properties could enhance its capability for photo catalytic degradation of pollutants or contaminants in water, contributing to improved water quality.

Acknowledgements

The authors are grateful to Noorul Islam Centre for Higher Education for their support in experimental works and characterization techniques

References

[1] Thavasi, V., Singh, G., & Ramakrishna, S., Energy & Environmental Science, 1(2), 205-221,(2008); https://doi.org/10.1039/b809074m

[2] Chen, H., Gao, Y., Li, J., Fang, Z., Bolan, N., Bhatnagar, A., Wang, H., Carbon Research, 1(1), 4,(2022); https://doi.org/10.1007/s44246-022-00005-5

[3] Jiang, Y., Shi, X., Feng, Y., Li, S., Zhou, X., Xie, X., Composites Part A: Applied Science and Manufacturing, 107, 657-664,(2018); https://doi.org/10.1016/j.compositesa.2018.02.016

[4] Tripathy, D. B., Mishra, A., Clark, J., Farmer, T., Comptes Rendus Chimie, 21(2), 112-130,(2018); https://doi.org/10.1016/j.crci.2017.11.005

[5] Caines, A. J., Haycock, R. F., Hillier, J. E. Automotive lubricants reference book (Vol. 354). John Wiley & Sons, (2004).

[6] Dupont, J., Scholten, J. D., Chemical Society Reviews, 39(5), 1780-1804, (2010); https://doi.org/10.1039/b822551f

[7] Kumar, A., Malik, G., Chandra, R., Mulik, R. S., Ceramics International, 46(13), 21800-21804, (2020); https://doi.org/10.1016/j.ceramint.2020.05.213

[8] Cassabois, G., Valvin, P., Gil, B., Nature photonics, 10(4), 262-266, (2016); https://doi.org/10.1038/nphoton.2015.277

[9] Fang, W., Li, Q., Li, J., Li, Y., Zhang, Q., Chen, R., Wang, T. (2023), Crystals, 13(6), 915,(2023); https://doi.org/10.3390/cryst13060915